Advances In Multidisciplinary & Scientific Research
A Multidisciplinary & Interdisciplinary Journal
AIMS Research Journal

Volume 8, No 2, June 2022 Series

Simultaneous Radial Distribution Network Reconfiguration and Distributed Generation Allocation using a Novel Adaptive Dingo Optimization Algorithm

Adeyemo, I.A., Oyedele, A.O., Salimon, S.A. & Adebiyi, O.W.
[1, 2, 3, 4] Department of Electronic & Electrical Engineering
Ladoke Akintola University of Technology
PMB 4000, Ogbomoso, Oyo State, Nigeria.
Emails:, iaadeyemo@lautech.edu.ng, oyedeleafeez1@gmail.com, sasalimon@lautech.edu.ng
owadebiyi@lautech.edu.ng

ABSTRACT

In this study, a novel swarm intelligence-based optimization technique called adaptive dingo optimization algorithm (DOA) is presented for the optimal reconfiguration of radial structure and allocation of distributed generation (DG) with the aim of power loss minimization and voltage stability enhancement. DOA is a metaheuristic algorithm inspired by the cooperative behavior of dingoes in a pack when hunting their prey. The adaptive and highly collaborative hunting steps of dingoes such as exploration, encirclement of prey and exploitation are mathematically modeled and deployed for the simultaneous restructuring as well as optimal sizing and placement type-1 DG in radial distribution networks (RDNs). In order to satisfy the radial constraints and reduce infeasible configuration in the optimization process, the concept of fundamental loop is used to pre-select the candidate branches for each tie switch (open branch) in the search space. The adaptive DOA is tested on IEEE 33-bus and 69-bus RDNs using six different events of RDNR and DG allocation. The results obtained for the six events show that the proposed method is highly efficient for solving nonlinear and complex combinatorial problems such as simultaneous RDNR and DG allocation in RDNs. The efficacy of the adaptive DOA is further validated with comparison of the obtained simulation results with the results reported for similar event cases using nature-inspired algorithms like uniform voltage distribution-based adaptive cuckoo search algorithm, Jaya algorithm, spring search algorithm and adaptive modified whale optimization algorithm. The comparative study shows that the adaptive DOA outperforms them in terms of power loss reduction and voltage profile improvement.

Keywords- Adaptive dingo optimization algorithm, DG allocation, radial distribution network, reconfiguration.

Aims Research Journal Reference Format:
Adeyemo, I.A., Oyedele, A.O., Salimon, S.A. & Adebiyi, O.W. (2022): Simultaneous Radial Distribution Network Reconfiguration and Distributed Generation Allocation using a Novel Adaptive Dingo Optimization Algorithm. Advances in Multidisciplinary and Scientific Research. Vol. 8. No. 3, Pp 13–38. www.isteams.net/aimsjournal. dx.doi.org/10.22624/AIMS/V8N3P2

1. INTRODUCTION

Electric power distribution network (DN) is the last link between the end-users of electricity and the transmission network. It consists of feeders made up of laterals and sub-laterals through which consumers are connected to the grid. Most distribution networks are eithers weakly meshed or radial in nature. Radial distribution network (RDN) is widely used due to its simplicity and cheap cost [1]. In RDN, there is unidirectional flow of power from the sub-station to every feeder in the network. However, RDN suffers from poor reliability, excessive voltage drops and significant power losses due to its high resistance to reactance ratio. Generally, the percentage of power losses is considerably higher in the distribution system than generation and transmission systems [2]. The summation of all losses at the distribution level is estimated to be about 13% of the total generated power while about 70% of the total losses in the electrical power system occur in the distribution network [3].

Despite the losses in the distribution network, the high cost of building new power plant and unabating increase in the global power demand have constrained the utility providers to heavily load the distribution network and operate very close to the limit of the network, which may eventually result in the network voltage collapse. In order to protect the network against voltage collapse, efforts are continually made to mitigate power losses and improve voltage profile using various methods such as load management, capacitor placement, network reconfiguration and distribution generation (DG) allocation [4].

Radial distribution network reconfiguration (RDNR) and distributed generation (DG) allocation are among the most effective methods for power loss reduction and performance enhancement of RDNs. RDNR is the process of altering the configuration of the sectionalizing switches (SS), which are the normally closed branches and the tie switches (TS) that are the normally open branches of the network such that an improved radial structure is obtained [5]. Alteration of the open/closed status of the switches changes the direction of power flow in the RDNs and facilitate load transfer among feeders. This alteration mostly results in reduction of power losses, more balanced feeder loads as well as improvement of voltage profile, stability and reliability [5].

Distributed generation on the other hand can simply be defined as electric power generation systems installed within distribution networks [6]. Based on their real and reactive power injecting capabilities, DG units are classified into four types. Type-1 DG only has real power injecting capability. Type-2 DG has the capability to inject both real and reactive power while type-3 can only inject reactive power. Similar to type-1, type- 4 has the capability to inject real power but it also consumes reactive power in the process. The benefits of optimal sizing and sitting of DG units in distribution network include significant power loss reduction and voltage profile enhancement. However, improper allocation of DG units may result in deterioration of the distribution network with the attendant higher power losses [6].

Optimal allocation of DG units in RDN while performing RDNR yields operational benefits such as higher power loss reduction and significant voltage profile improvement. The choice of DG type, sizing and sitting in radial distribution network is a complex and nonlinear combinatorial optimisation problem that is exacerbated when combined with RDNR. Using different objective functions such as percentage power loss reduction index (%PLRI), voltage stability index (VSI), loss sensitivity factor (LSF) etc, several analytical methods as well as nature-inspired optimization techniques have been proposed for solving the combinatorial optimization problem with varying degrees of accuracy and efficiency.

Using a multi-objective function that consists of power loss reduction, voltage profile enhancement as well as mitigation of current and voltage unbalance problems, the authors in [5] solved the RDNR and DG allocation problem in balanced and unbalanced networks using genetic algorithm (GA). With the objective of minimizing both power loss and voltage deviation, Sambaiah and Jayabarathi proposed salp swarm algorithm (SSA) for solving the combinatorial problem [7]. The authors tested the proposed SSA on 33-bus and 69-bus RDNs using five event cases. By considering different models of DG with the aim of real power loss reduction, Guan *et al* presented decimal coded quantum particle swarm optimization (DQPSO) for RDNR and DG allocation [8].

Using multi-objective function that consists of reduction of power losses, cost of operation and emission of pollutant gas coupled with maximization of VSI, Esmaeili *et al* implemented hybrid bang-big crunch (MOHBB-BC) for optimal RDNR and DG allocation on balanced and unbalanced RDNs [9]. In [10], a non-dominated sorting particle swarm optimization (NSPSO) approach has been presented for solving the combinatorial problem with the objective of network performance improvement, minimization of real power loss and voltage deviation as well as mitigation of renewable energy wastage. Moth-flame optimization (MFO) algorithm has been used to solve the combinatorial optimization problem in [11]. The approach results in real power loss reduction, voltage profile improvement, reliability and stability enhancement. Teaching learning-based optimization (TLBO) has also been used to solve the problem in [12] and [13] for the maximization of annual energy loss reduction and loadability of RDN, respectively.

Biswas *et al* [14] have presented LSHADE-EpSin algorithm with encouraging results for simultaneous optimization of RDNR, capacitor and DG allocation for real power loss minimization. By considering the effect of different voltage dependent load models, an improved elistist-jaya algorithm is proposed in [15] for RDNR and DG allocation. In [16], an improved equilibrium optimization algorithm (IEOA) along with a recycling strategy is presented for RDNR and DG allocation with both real power loss and voltage profile improvement as the objective function. Abdelkader *et al* [17] have presented an analytical approach to RDNR and DG allocation for the reduction of real power loss. For the mitigation of real power loss and voltage stability,

Raut and Mishra developed an improved sine-cosine algorithm (ISCA) for the simultaneous implementation of RDNR and DG allocation [18]. Optimal allocation of DG and RDNR using modified marine predator optimizer (MMPO) is presented in [19]. In [20], enhanced sine-cosine algorithm (ESCA) is utilized to solve the RDNR and DG allocation problem with the objective of minimizing real power loss and operation cost. In [21], butterfly optimization (BO) has been proposed for RDNR and DG allocation to enhance the RDN loadibility and real power loss reduction. Shaheen *et al* [22] developed artificial ecosystem optimizer (AEO) for RDNR, capacitor and DG allocation to minimize real power loss. In [23], Bagheri *et al* presented tabu search algorithm (TSA) for solving the RDNR and DG allocation problem considering switching cost, losses cost and reactive power generation of DGs.

Using different combinations of RDNR and DG allocation, Nguyen *et al* [24] proposed adaptive cuckoo search algorithm (ACSA) for solving the combinatorial problem with the mitigation of real power loss and voltage stability enhancement as the objective function. Several other optimization techniques such as harmony search algorithm (HSA) [25], fireworks algorithm (FWA) [26], firefly algorithm (FFA) [27], modified plant growth algorithm (MPGA) [28], grasshopper optimization algorithm (GOA) [29], uniform voltage distribution-based constructive reconfiguration algorithm (UVDA) [30], spring search algorithm (SSA) [31] and adaptive modified whale optimization algorithm (AMWOA) [32] with problem formulation and objective function similar to [24] have been deployed for the optimization of RDNR and DG allocation.

Most these works considered real power loss reduction as their objective function. However, in [26] and [32], voltage stability is considered alongside the power loss reduction using weighted average method while voltage deviation and real power loss are considered in [31]. Three heuristic optimization techniques: integrated particle swarm optimization (IPSO), teaching learning-based optimization (TLBO) and Jaya optimization are proposed for the optimisation of RDNR and DG allocation in [33] with the goal of real power loss minimization and voltage stability improvement. Hybridized grey wolf optimizer and particle swarm optimizer (GWO-PSO) is proposed in [34] for RDNR and DG allocation with the goal of real power loss minimization.

In this study, a novel adaptive dingo optimization algorithm (DOA) is presented for simultaneous radial distribution network reconfiguration and DG allocation. The proposed adaptive DOA uses real power loss reduction as the objective function to find the optimal configuration of radial distribution networks and also optimize the sizing and placement of DG units in the networks.

2. PROBLEM FORMULATION

2.1 Objective Function and Constraints

The main purpose of simultaneous reconfiguration of RDN and DG allocation is total real power loss reduction in the network. Hence, this is considered as the objective function of this work. The total real power loss of any RDN is the summation of all the real power losses in the line sections of the system:

$$OF_{min} = RP_{loss} = \sum_{i}^{n_b} |I_i|^2 R_i \tag{1}$$

Here, OF_{min} denotes the objective function, which is minimization of total real power loss (RP_{loss}), n_b is the total number of branches in the RDN, R_i is the resistance of the i^{th} branch of the RDN and $|I_i|$ is the current magnitude of the i^{th} branch of the RDN.

2.2 Constraints

In this study, simultaneous RDNR and DG is formulated as a combinatorial optimisation problem in which the objective function is minimization of total real power loss subject to the following constraints:

2.2.1 Power flow equations

The power flow equation is solved using the Newton Raphson load flow technique in the optimization process. These equations are given as:

$$P_{gi} = P_{di} + \sum_{j=1}^{n_b} |V_i| \left|V_j\right| \left[G_{ij} \cos\theta_{ij} + B_{ij} \sin\theta_{ij}\right] \quad (2)$$
$$Q_{gi} = Q_{di} + \sum_{j=1}^{n_b} |V_i| \left|V_j\right| \left[G_{ij} \cos\theta_{ij} - B_{ij} \sin\theta_{ij}\right] \quad (3)$$

Where
V_i and V_j are the voltages of buses 'i' and 'j' respectively; P_{gi} and P_{di} are the real power generated and power demanded at bus 'i'; Q_{gi} and Q_{di} are the reactive power generated and demanded at bus 'i'; and θ_{ij} is the difference between the voltage angles of buses 'i' and 'j'.

2.2.2 Real Power Generation Constraint of DG
The size of the each of the installed DG is constrained within the limits in (4);

$$P_{DG(min)} \leq P_{DG} \leq P_{DG(max)} \quad (4)$$

Where
$P_{DG(min)}$= 100 kW and $P_{DG(max)}$ is 75% of the total real power demand of the network.

2.2.3 Bus voltage limitation
The voltage at each of the buses in the RDN is constrained within the specified limits

$$V_{min} \leq V_i \leq V_{max} \quad (5)$$

Where
V_i is the bus voltage, V_{min} and V_{max} are the permissible minimum and maximum voltage limit, respectively. In this study, V_{min}= 0.95 p.u. and V_{max} = 1.05 p.u.

2.2.4 DG penetration limitation
The total real power supplied by the installed DG must be less than 75% of the total real power demand of the network [35].

$$\sum_{l=1}^{m} P_{DG}(l) \leq 0.75 \times \sum_{i=1}^{n_b} P_d(i) \quad (6)$$

2.2.5 Radial Configuration Constraint
The radial nature of the RDN must be maintained such that there is only a unidirectional flow of power to all the buses associated with the network except the slack bus.

2.3 Performance evaluation indices
In order to assess the effectiveness of the proposed technique, some performance evaluation metrics are used as benchmark parameters for comparison of various events and other techniques in open literature. The performance evaluation metrics are:

2.3.1 Real power loss ($\boldsymbol{RP_{loss}}$) and percentage power loss reduction index (%$\boldsymbol{PLRI}$)
The real power loss is the total of all the real power losses in all the lines of the RDN as given in equation (1). The main goal of the optimization process in optimal reconfiguration is to minimize real power loss. In order to have a fair comparison with other techniques which may have their base case

$RP_{loss(before\_rec\_DG)}$ different from the one used in the study, the percentage power loss reduction index is calculated as given below:

$$\%PLRI = \frac{RP_{loss(before\_rec\_DG)} - RP_{loss(after\_rec\_DG)}}{RP_{loss(before\_rec\_DG)}} \times 100\% \quad (7)$$

Where

$RP_{loss(before\_rec\_DG)}$ and $RP_{loss(after\_rec\_DG)}$ are the power losses of the RDN before and after simultaneous RDNR and DG allocation, respectively.

2.3.2 Voltage profile and minimum voltage

Voltage profile is the voltage of all the buses of the RDN after performing load flow while minimum voltage (V_{min}) denotes voltage of the bus with the least value.

2.3.3 Voltage stability index (VSI) and minimum VSI ($\boldsymbol{VSI_{min}}$)

RDNs are vulnerable to voltage instability and collapse when overloaded and operated under stress. The VSI is used to identify buses that are close to the point of collapse and may need compensation [36]. It is given as follows:

$$VSI = |V_s|^4 - 4[P_r R_{sr} + Q_r X_{sr}]|V_r|^2 - 4[P_r R_{sr} + Q_r X_{sr}] \quad (8)$$

Where

s and *r* stand for the sending and receiving end bus. V, P, and Q represent voltage magnitude, real and reactive power, respectively. R and X represent the resistance and reactance between the sending and receiving bus. The least value of the VSI in the RDN is referred to as the minimum VSI (VSI_{min}) and the bus having the minimum VSI is the most susceptible to the voltage collapse.

3. DINGO OPTIMIZATION ALGORITHM (DOA)

Dingo optimization algorithm proposed by Bairwa *et al* in 2021 is a nature-inspired metaheuristic optimization technique that is based on the prey hunting behavior of dingoes in a pack [37]. Dingoes are highly intelligent and social animals that live in a pack of about 12 -15. They have a well-developed sense of communication, which they exhibit during their adaptive, skillful and collaborative group hunting of preys. In a pack of dingoes, there is a well-structured social hierarchy. The leader of the pack, called alpha is usually the strongest and most dominant member of the pack. It has the responsibility to make decisions that are binding on all members of the pack. Next to the alpha in the chain of command is beta dingo. Beta dingo maintains discipline in the group and plays an intermediary role between the alpha and other members of the group that are referred to as subordinates. If alpha dingo is severely wounded or killed, the mantle of leadership automatically falls on the beta dingo. Generally, subordinate dingoes approach a more dominant dingo in a crouched posture with their tails down.

All other dingoes support the alpha and beta to catch prey and provide food for the pack. The steps involved in the group hunting of preys by dingoes are: searching, encircling, hunting and attacking the prey. The steps are mathematically modeled using equations (9) – (13) [37].

$$\vec{D}_d = \left|\vec{A} \cdot \vec{P}_p(x) - \vec{P}(i)\right| \tag{9}$$
$$\vec{P}(i+1) = \vec{P}_p(i) - \vec{B} \cdot \vec{D}(d) \tag{10}$$
$$\vec{A} = 2 \cdot \vec{a}_1 \tag{11}$$
$$\vec{B} = 2\vec{b} \cdot \vec{a}_2 - \vec{b} \tag{12}$$
$$\vec{b} = 3 - \left(I * \left(\frac{3}{I_{max}}\right)\right) \tag{13}$$

Where $\vec{D}_d$ is the distance between the dingo and prey; $\vec{P}_p$ is position vector (prey); $\vec{P}$ is position vector (dingo); $\vec{A}$ and $\vec{B}$ are vector coefficients; $\vec{a}_1$ and $\vec{a}_2$ are random vector in $[0,1]$, the value of $\vec{b}$ linearly decreases from 3 to 0 during every iteration.

(i) Searching: All dingoes have an innate ability to locate preys and they are always forward moving when hunting their preys. The group hunting of prey by dingoes starts with a search of their territory for preys. Each of the dingoes has the capability to locate the prey in the search space. Vector coefficients $\vec{A}$ and $\vec{B}$ in equations (9) and (10) are the components of DOA that ensure global exploration. $\vec{A}$ is the vector coefficient that is responsible for the random selection of preys by assigning randomly generated number in the interval of [0, 3] as weight to the arbitrarily chosen preys. The stochastic exploration values provided by $\vec{A}$ during iterations ensures the global exploration of the search space, and protects the solution from getting trapped in local optima. $\vec{B}$ is the vector coefficient that deals with the direction of movement of dingoes with respect to the position of prey or predator. It guides the pack to prey and also enables the pack to avoid predator. It is assigned any random number such that when $\vec{B}$ is less than -1, it means that the distance between prey and the search agent is increasing but if the value is greater than 1, it means that their distance apart is decreasing and the pack is moving closer to the prey.

(ii) Encircling: In the mathematical modeling of dingoes, it is assumed that the group has an idea of the potential location of the prey. The alpha dingo directs and sometimes participate in the hunting process. After searching and detecting the prey's location, the alpha commands the other dingoes to encircle the prey [37]. Each dingo randomly changes its location with respect to the prey's position inside the search space by changing its values of $\vec{A}$ and $\vec{B}$ according to equations (11) and (12).

(iii) Hunting: Based on the location of the best search agent, all other dingoes randomly update their respective position with respect to the position of the prey in the search space. The dingoes update their positions according to equations (14) – (22) [37].

$$\vec{D}_\alpha = \left|\vec{A}_1 \cdot \vec{P}_\alpha - \vec{P}\right| \tag{14}$$
$$\vec{D}_\beta = \left|\vec{A}_2 \cdot \vec{P}_\beta - \vec{P}\right| \tag{15}$$
$$\vec{D}_o = \left|\vec{A}_3 \cdot \vec{P}_o - \vec{P}\right| \tag{16}$$

$$\vec{P}_1 = \left|\vec{P}_\alpha - \vec{B}\cdot\vec{D}_\alpha\right| \quad (17)$$
$$\vec{P}_2 = \left|\vec{P}_\beta - \vec{B}\cdot\vec{D}_\beta\right| \quad (18)$$
$$\vec{P}_3 = \left|\vec{P}_o - \vec{B}\cdot\vec{D}_o\right| \quad (19)$$

The following equations are used to estimate the intensity of each dingo

$$\vec{I}_\alpha = log\left(\frac{1}{F_\alpha-(1E-10\ \ )} + 1\right) \quad (20)$$
$$\vec{I}_\beta = log\left(\frac{1}{F_\beta-(1E-100)} + 1\right) \quad (21)$$
$$\vec{I}_o = log\left(\frac{1}{F_o-(1E-10\ \ )} + 1\right) \quad (22)$$

(iv) Attacking prey: If there is no update on position, it means a dingo has successfully attacked the prey. The value of $\vec{b}$ in equation (13) is linearly decreased from 3 to 0 to model this strategy. DOA terminates itself whenever any of the termination criteria is satisfied.

3.1 Adaptive DOA for RDNR and DG allocation

The radiality constraints imposed on the simultaneous RDNR and DG allocation optimization problem results in a number of infeasible configurations during the initialization and intermediate stages. This occurs because a number of sectionalizing switches (SS) will form the search agents (dingoes) in the population, such that when they are opened (or turned to TS) may result in a non-radial structure or infeasible configuration. Hence, In the proposed adaptive dingo optimization algorithm (DOA), the dingoes (search agents) are generated using graph theory to minimize the number of infeasible configurations at every stage of the optimization process.

3.2 Adaptation of DOA Through Graph Theory For Removal Of Infeasible Configuration

In the conventional DOA proposed by Bairwa *et al* [37], there is a random generation of the initial population of dingoes. However, such approach for simultaneous RDNR and DG allocation optimization results into a large number of infeasible configurations that are unable to satisfy the radiality constraints. This problem is mitigated using the concept of fundamental loop. The infeasible configurations are reduced in the adaptive DOA with the graph theory in such a way that only switches belonging to the fundamental loops are generated. Using line data of the RDN, the process starts with the formation of an incidence matrix C, which has one row for each branch and one column for each bus with an entry c_{ij} in row *i* and column *j* according to the following rules [38]:

$$c_{ij} = \begin{cases} +1\ for\ a\ branch\ i\ directed\ away\ from\ node\ \text{j} \\ -1\ for\ a\ branch\ i\ directed\ \text{toward}\ node\ \text{j} \\ 0\ for\ a\ branch\ i\ \text{not connected to}\ node\ \text{j} \end{cases}$$

(23)

Fundamental loops (FLs) are formed in the network when all the tie switches (TS) of the RDN are closed. The number of fundamental loops formed in the RDN is the same as the number of TS [39, 40]. To determine the FLs of an RDN, a tie switch (TS) is added to the incidence matrix.

The absolute sum of the corresponding column S_C of the matrix after addition of a tie switch is calculated using the technique utilized in [24]. The branches connected to bus whose S_C is 1 are removed. This process is repeated until all the branches connected to bus whose S_C are 1 are no longer available in the RDN. The number of branches remaining forms a fundamental loop (FL), which is saved [40]. Thereafter, another TS is added and the whole process repeated. Figure 1 shows a simple sample of RDN with TSs and the first FLs are determined as depicted in Figure 2.

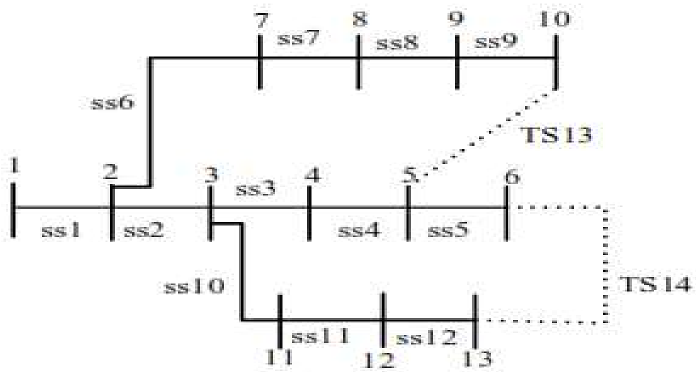

Figure 1. A simple sample of 13-bus RDN

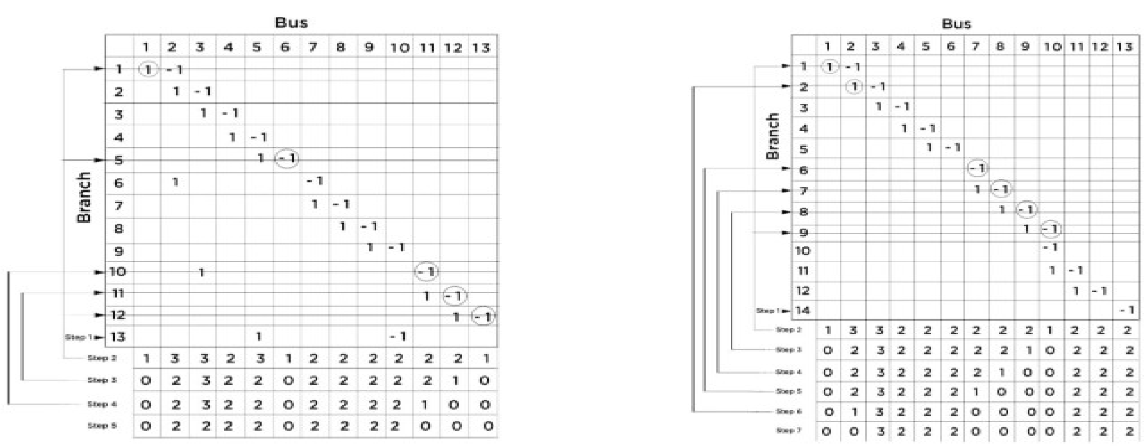

Figure 2. Determination of FLs when closing branches (a) 13 (b) 14

As shown in Figure 2, after determining the incidence matrix, the following steps are executed to identify the first FLs. The flowchart for determining the fundamental loops of the RDN is shown in Figure 3. Each radial configuration which involves a set of open branches are randomly chosen from corresponding FLs. This helps to reduce the generation of infeasible configuration during each stage of the optimization algorithm. However, some of the branches are common in some of FLs [40]. Therefore, radial condition of network must be checked.

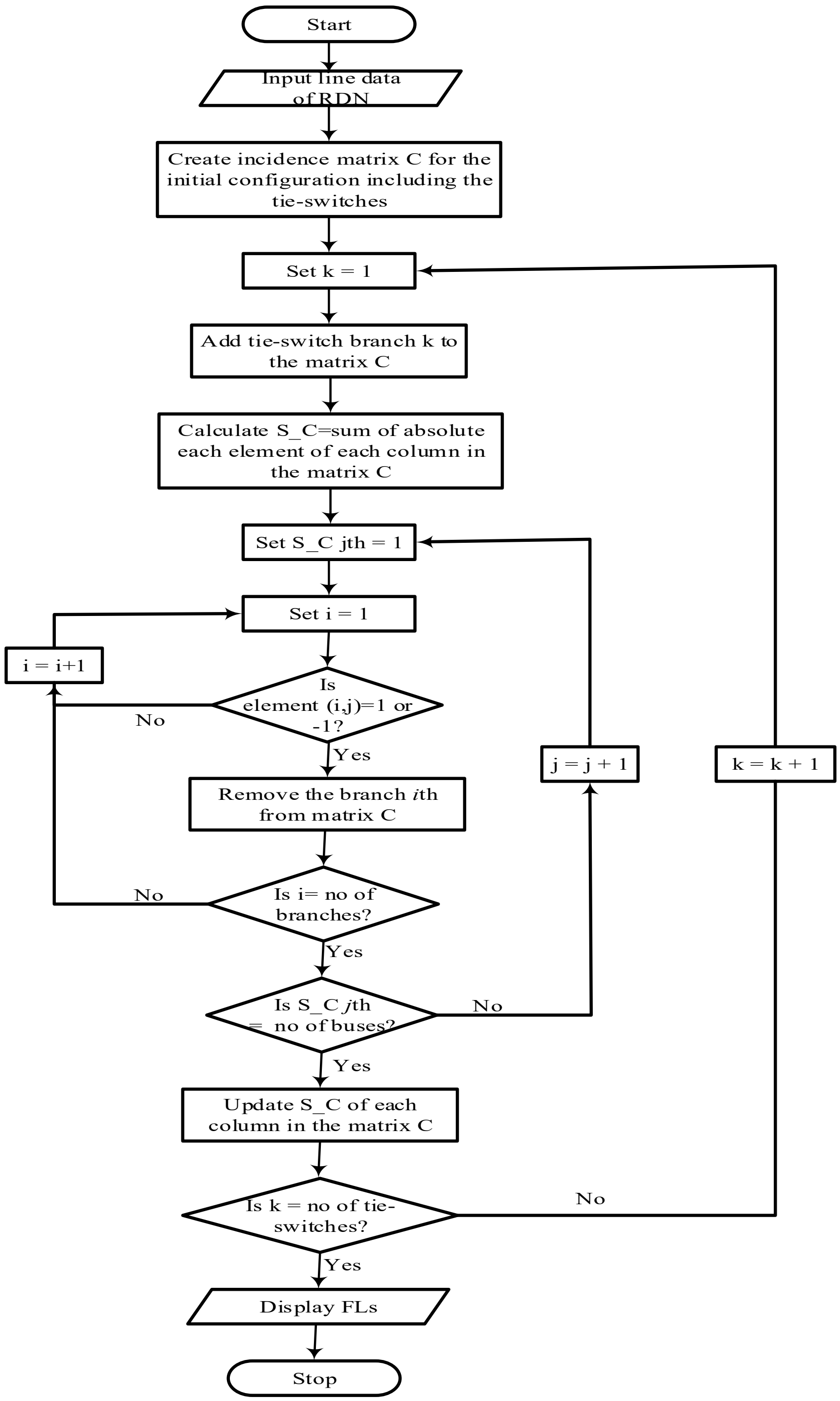

Figure 3. Flowchart for finding fundamental loops (FLs) of any RDN

3.3 Radial configuration check

In order to satisfy the radial configuration constraints, a radial configuration check is conducted before performing load flow and obtaining the fitness function of each generated solution at various stages of the optimization process of the proposed technique. In each configuration, the incidence matrix C is determined. Then, the first column corresponding to the slack bus in the RDN will be removed to form a square matrix C. If the configuration is radial, the determinant of square matrix C is equal to ± 1, otherwise the configuration is non-radial [38]. The flowchart for the radial feasibility of the configuration is shown in Figure 4.

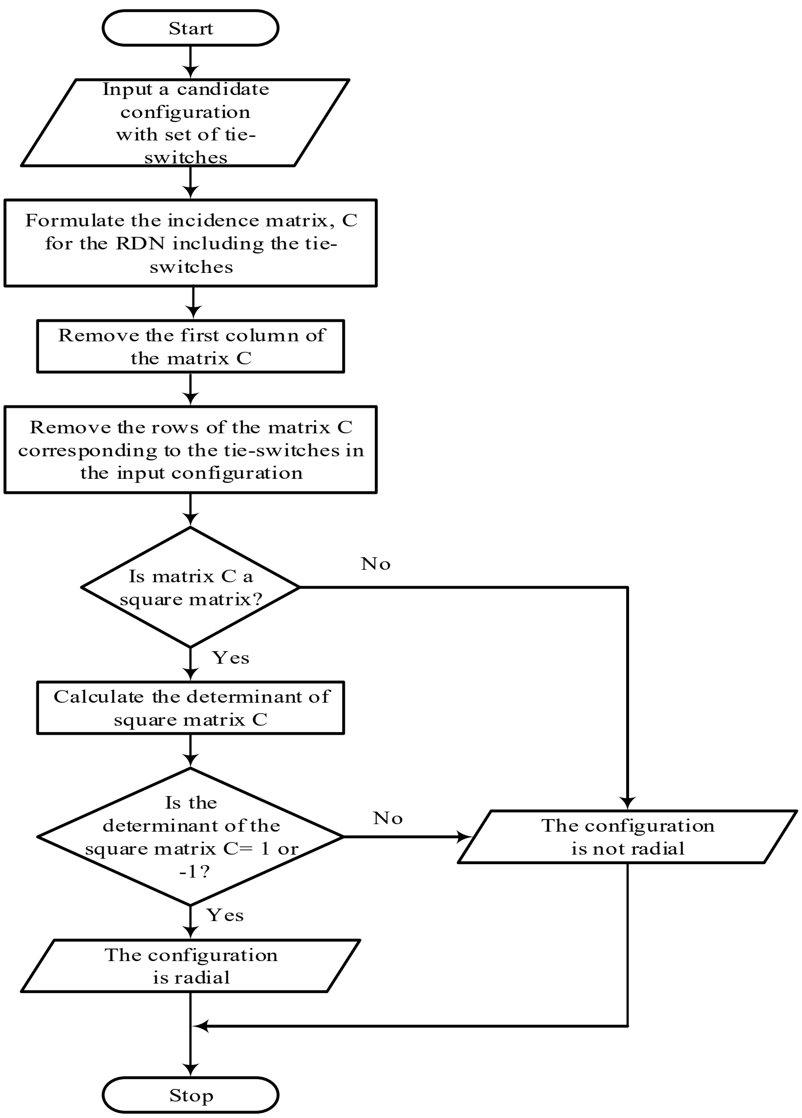

Figure 4. Radiality check for candidate configuration

3.4 Application of DOA for simultaneous RDNR and DG allocation

The DOA technique is implemented for solving the RDNR and DG allocation problem using the following steps:

Step 1: Input the line and load data of the RDN including the tie switches, and DOA parameters.
Step 2: Obtain the fundamental loops (FLs) of the RDN using steps given in Figure 3.
Step 3: Determine the upper-bound and lower-bound of each tie-switch based on the size of the branches that constitute it corresponding to FLs.
Step 4: Subject to radiality check in order to reduce infeasible configurations, an initial population of dingoes is generated as explained in section 3.2. In the application of the DOA technique, each dingo is a potential solution that consists of radial configuration, DG locations and DG sizes. A population of *n* dingoes is represented as:

$$D = \begin{bmatrix} D_1 \\ D_2 \\ \vdots \\ D_n \end{bmatrix} = \begin{bmatrix} TS_1^1,\dots,TS_{NTL}^1 & bus.DG_1^1,\dots,bus.DG_m^1 & cap.DG_1^1,\dots,cap.DG_m^1 \\ TS_1^2,\dots,TS_{NTL}^2 & bus.DG_1^2,\dots,bus.DG_m^2 & cap.DG_1^2,\dots,cap.DG_m^2 \\ \vdots\ddots\ddots\ddots\ddots\ddots\vdots & \vdots\ddots\ddots\ddots\ddots\ddots\vdots & \vdots\ddots\ddots\ddots\ddots\ddots\vdots \\ TS_1^n,\dots,TS_{NTL}^n & bus.DG_1^n,\dots,bus.DG_m^n & cap.DG_1^n,\dots,cap.DG_m^n \end{bmatrix} \tag{24}$$

Each dingo in the population can be represented as:

$$D_i = [TS_1^i, \dots, TS_{NTL}^i \quad bus.DG_1^i, \dots, bus.DG_m^i \quad cap.DG_1^i, \dots, cap.DG_m^i]` \tag{25}$$

It can be seen from equation (25) that the solution vector of each dingo contains three parts. The first part represents the number of tie switches or lines (open branches) of the RDN, the second part represent the number of buses selected for DG integration and the third part stands for the capacities (sizes) of the DG units. In the equations, $TS_1, TS_2, \dots, TS_{NTL}$ are the tie switches or lines (open branches) in the fundamental loops, $FL_1$to FL_{NTL}; $bus.DG_1, bus.DG_2, \dots, bus.DG_m$ are the buses chosen for the placement of DG; $cap.DG_1, cap.DG_2, \dots, cap.DG_m$ are the sizes (or capacities) of the DG units in kW to be installed at the buses, respectively.

Therefore, each dingo, D_i of the population is randomly initialized as follows:

$$TS_i = round\left[TS_{lower,r1}^i + rand \times (TS_{upper,r1}^i - TS_{lower,r1}^i)\right] \tag{26}$$

$$bus.DG_i = round\left[bus_{lower,r2}^i + rand \times (bus_{upper,r2}^i - bus_{lower,r2}^i)\right] \tag{27}$$

$$cap.DG_i = round\left[cap_{lower,r3}^i + rand \times (cap_{upper,r3}^i - cap_{lower,r3}^i)\right] \tag{28}$$

Where
r_1= 1, 2, . . . NTL, r_2= 1, 2, . . .m and r_3= 1, 2 . . . m. $TS_{lower,r1}$ and $TS_{upper,r1}$ are the minimum and the maximum tie-switch, respectively which are encoded in the fundamental loop r_1. DGs are placed on any bus of the RDN apart from the slack bus, which represent the first bus. Hence, the lower limit ($cap_{lower,r2}$) and upper limit ($cap_{upper,r2}$) for the placement of the DG units is from bus 2 to the last bus of the RDN and the capacities of each DG is from 100 kW to maximum power of DG as given in the inequality constraint of equation (4).

Step 5: For i = 1:D_n, perform the radial configuration check and fitness evaluation for each of the dingoes. The fitness function of non-radial configuration is set at infinity. The load flow is performed for each of the dingoes using Newton Raphson technique to determine the fitness function which is taken as the power loss in this study.

Depending on the values of the fitness function (power loss), the following are obtained:

(i) the Dingo with the best search (D_a)
(ii) the Dingo with the second-best search (D_b)
(iii) the Dingo search results afterwards (D_c)

Step 6: Based on the location of the best search agent, update the positions of the search agent (dingoes) using equations (14) – (19).
Step 8: Record the best values of D_a, D_b and D_c as well as the values of $\vec{b}$, $\vec{A}$, and $\vec{B}$
Step 9: Repeat steps 4 - 8 until the maximum number of iteration ($iter_{max}$) is reached or any of the termination criteria is satisfied.
Step 10: Print the best dingo.

4. RESULTS AND DISCUSSION

The efficacy of the adaptive DOA technique in solving the simultaneous RDNR and DG allocation is tested on the IEEE 33-bus and 69-bus RDNs using a personal computer with the following specifications: 64-bit operating system, 2.11 GHz, core i5 and 8 GB RAM running MATLAB R2021a on Windows 10 Pro. The line and load data of the two test RDNs are found in [41, 42].

The 33-bus RDN consist of 37 branches made up of 32 sectionalizing switches (SS), 5 tie switches (TS) while the 69-bus RDN consist of 73 branches made up of 68 sectionalizing switches (SS) and 5 tie switches (TS). In this study, the total number of allocated DG is limited to three. The parameters of the DOA utilized in the study are population, D_n = 1000, and maximum number of iterations, $iter_{max}$ is 200.

To validate the superiority of DOA, six different events are considered as follows:
Event 1: Base case (BC) without RDNR and DG allocation
Event 2: Reconfiguration (RDNR) only
Event 3: DG allocation only
Event 4: DG allocation after reconfiguration of the network
Event 5: Reconfiguration (RDNR) after DG allocation on the RDN
Event 6: Simultaneous RDNR and DG allocation

4.1 IEEE 33-bus RDN

IEEE 33-bus RDN has a voltage of 12.66kV, real and reactive load size of 3.715MW and 2.3MVar, respectively. The fundamental loops obtained for the 33-bus RDN are shown in Table 1. The branches shown in the table give the boundary and limits of the possible open branches for each of the FLs.

Advances In Multidisciplinary & Scientific Research
AIMS Research Journal
A Multidisciplinary & Interdisciplinary Journal
Volume 8, No 2, June 2022 Series

Table 1. Fundamental loops (FLs) of the IEEE 33-bus RDN

FL Number	Branches
FL_1	2, 3, 4, 5, 6, 7, 18, 19, 20, 33
FL_2	9, 10, 11, 12, 13, 14, 34
FL_3	2, 3,4, 5, 6, 7, 8, 9, 10, 11, 18, 19, 20, 21, 35
FL_4	6, 7, 8, 9, 10, 11, 12, 13, 14, 15, 16, 17, 25, 26,27, 28, 29, 30, 31, 32, 36
FL_5	3, 4, 5, 22, 23, 24, 25, 26, 27, 28, 37

The results obtained for all the considered cases for the 33-bus RDN are given in Table 2.

Table 2. Summary and comparison of results for the various events for the 33-bus RDN

Event/item	Adaptive DOA	UVDA [30]	ACSA [24]	JAYA [33]	SSA [31]	AMWOA [32]
Base case						
TS	33, 34, 35,36,37	33,34,35,36 ,37	33,34,35,36 ,37	33,34,35,36 ,37	33,34,35,36 ,37	33,34,35,36 ,37
RP_{loss} (kW)	202.70	202.69	202.68	202.67	202.66	202.32
V_{min} (p.u.)	0.9131 (18)	0.9131 (18)	0.9108	0.9131	0.9131 (18)	-------
VSI_{min} (p.u)	0.6956	-------	0.6978	0.6951	-------	0.696
RDNR only						
TS	7, 9, 14, 28, 32	7, 9,14, 32, 37	7, 14, 9, 32, 28	7 9 14 28 32	7 9 14 32 37	7 9 14 28 32
RP_{loss} (kW)	139.997	139.55	139.98	139.98	139.55	139.74
%PLRI	**30.94**	**31.15**	**30.93**	**30.93**	**31.14**	**30.93**
V_{min} (p.u.)	0.9413 (32)	0.9378 (32)	0.9413	0.9413	0.9378 (32)	-------
VSI_{min} (p.u)	0.7850	-------	0.7878	0.7850	-------	0.787
DG only						
TS	33,34,35,36 ,37	33,34,35,36 ,37	33,34,35,36 ,37	33,34,35,36 ,37	33,34,35,36 ,37	33,34,35,36 ,37
DG size in kW (bus no)	754 (14) 1101 (24) 1073 (30)	875 (11) 931 (24) 925 (29)	779.8 (14) 1125.1 (24) 1349.6 (30)	762.8 (14) 1107.2 (24) 1280.9 (30)	753.6 (13) 1100.4 (23) 1070.6 (29)	808.6 (14) 1106.6 (24) 1338.3 (30)
RP_{loss} (kW)	71.47	74.21	74.26	72.95	71.45	71.70
%PLRI	**64.74**	**63.39**	**63.26**	**64.01**	**64.74**	**64.56**
V_{min} (p.u.)	0.9681 (33)	0.962 (33)	0.9778	0.9754	0.9686 (32)	-------
VSI_{min} (p.u)	0.8803	-------	0.9118	0.9054	-------	0.9297

DG after RDNR						
TS	7,9,14,28,32	7,9,14,32,37	7, 14, 9, 32, 28	7 9 14 28 32	7 9 14 32 37	7 9 14 28 32
DG size in kW (bus no)	929 (8) 1068 (24) 946 (30)	526 (12) 592 (15) 1125 (30)	1753.6 (29) 539.7 (12) 504.5 (16)	587.9 (12) 513.3 (16) 1659 (30)	932 (8) 1068 (24) 950 (30)	1530.1 (15) 580.7 (23) 461.2 (29)
RP_{loss} (kW)	58.07	66.60	58.79	60.86	58.87	57.64
%PLRI	**71.35**	**67.14**	**71.00**	**69.97**	**70.95**	**71.51**
V_{min} (p.u.)	0.9744 (32)	0.9758 (32)	0.9802	0.9835	0.9741 (33)	------
VSI_{min} (p.u)	0.9010	------	0.9264	0.9355	------	0.9318
RDNR after DG						
TS	7, 8, 9, 32, 37	------	33, 9, 8, 36, 27	8 9 26 33 36	7 8 28 32 34	8 9 26 33 36
DG size in kW (bus no)	754 (14) 1101 (24) 1073 (30)	------	779.8 (14) 1125.1 (24) 1349.6 (30)	762.8 (14) 1107.2 (24) 1280.9 (30)	753.6 (13) 1100.4 (23) 1070.6 (29)	808.6 (14) 1106.6 (24) 1338.3 (30)
RP_{loss} (kW)	57.52	------	62.98	60.85	58.37	60.89
%PLRI	**71.62**	------	**68.93**	**69.97**	**71.19**	**69.90**
V_{min} (p.u.)	0.9717 (33)	------	0.9826	0.9811	0.9690 (33)	------
VSI_{min} (p.u)	0.8982	------	0.9354	0.9266	------	0.9411
RDNR and DG						
TS	11, 28,31,33,34	7, 10, 13, 27, 32	33, 34,11, 31,28	9 13 28 30 33	6 14 11 17 28	11 28 31 33 34
DG size in kW (bus no)	949 (7) 752 (17) 1287 (25)	649 (15) 486 (21) 1554 (29)	896.8 (18) 1438.1 (25) 964.6 (7)	745 (9) 801 (18) 1215 (25)	1027 (8) 1180 (24) 837 (31)	829.9 (8) 1341.2 (17) 710.9 (31)
RP_{loss} (kW)	50.72	57.27	53.21	58.49	56.42	50.61
%PLRI	**74.98**	**71.74**	**73.75**	**71.14**	**72.16**	**74.98**
V_{min} (p.u.)	0.9734 (32)	0.976 (32)	0.9806	0.9813	0.9762 (18)	------
VSI_{min} (p.u)	0.8977		0.9318	0.9297	------	0.9066

As shown in the table, the power loss (in kW) for the BC event is 202.70. The initial power loss is significantly reduced to 139.997, 64.74, 58.07, 57.52 and 50.72 for events 2, 3, 4, 5 and 6, respectively; and has a corresponding percentage power loss reduction (%PLR) of 30.94, 64.74, 71.35, 71.62 and 74.89. A comparative study of the six events reveals that event 6 (simultaneous RDNR and DG allocation) has the least power loss closely followed by events 5 and 4. This clearly demonstrates the superiority of simultaneous RDNR and DG allocation to the other approaches in terms of power loss reduction capability and efficiency. As shown in Table 2, the minimum voltage significantly improved for all the considered events compared to the BC.

The minimum voltage (bus location) increased from 0.9131 (18) to 0.9413 (32), 0.9681 (33), 0.9744 (32), 0.9717 (33) and 0.9734 (32) for events 2 to 6, respectively. Similarly, the minimum voltage stability index (VSI_{min}), which is one of the performance evaluation metrics improved from 0.6956 (18) to 0.7858 (33), 0.8803 (33), 0.9010 (32), 0.8982 (33) and 0.8977 (32) for events 2 to 6, respectively. The voltage profiles and VSIs for all the considered events are displayed in Figures 5 and 6, respectively. It is clear from the figures that the bus voltages and VSIs are significantly improved after RDNR and DG allocation.

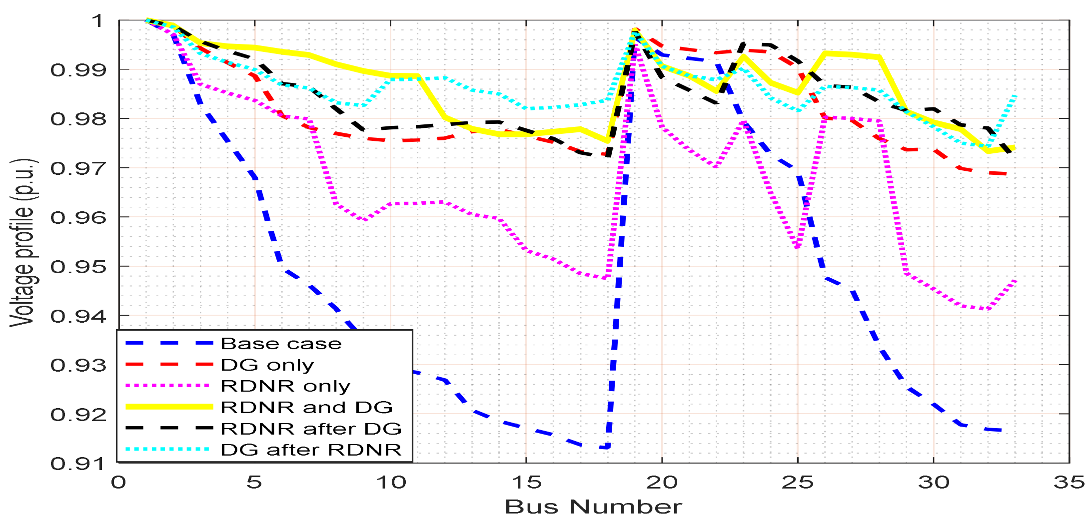

Figure 5. Voltage profile of events 1 – 6 for 33-bus RDN

Advances In Multidisciplinary & Scientific Research
AIMS Research Journal
A Multidisciplinary & Interdisciplinary Journal
Volume 8, No 2, June 2022 Series

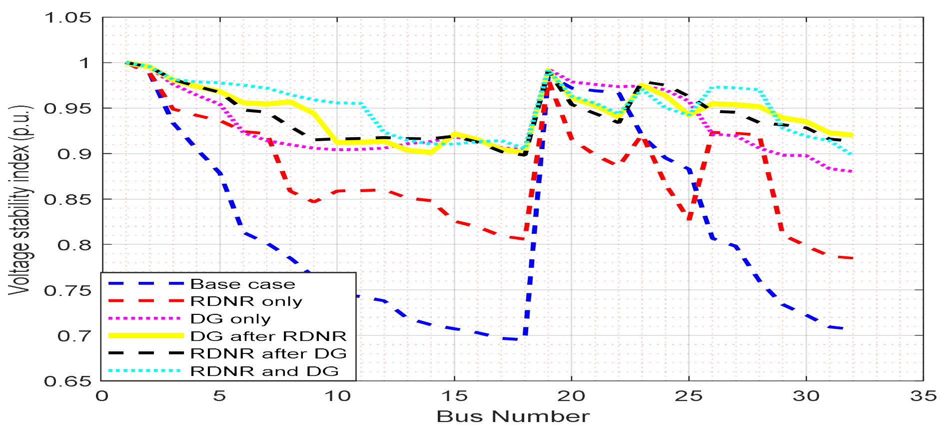

Figure 6. Voltage stability indices (VSIs) for events 2 – 6 for 33-bus RDN

The convergence characteristics of events 2 to 6 are illustrated in Figure. 7

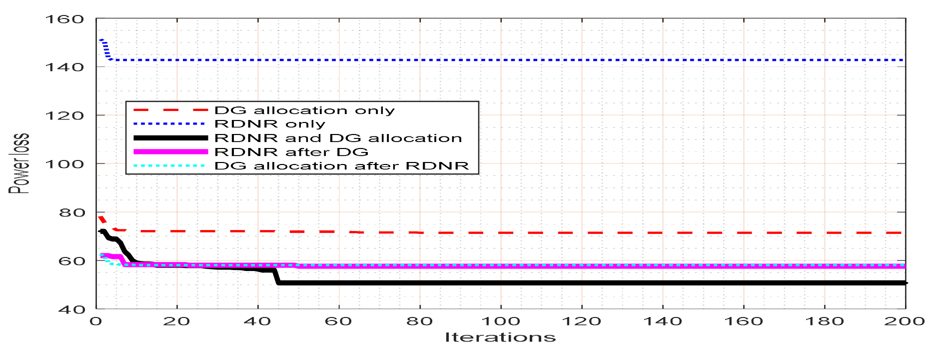

Figure 7. Convergence characteristics of events 2 – 6 for 33-bus RDN

The performance of the adaptive DOA technique is objectively compared with the results of recent literatures that considered the same events and the results are also presented in Table 2. The compared techniques used to validate the proposed method include adaptive cuckoo search algorithm (ACSA) [24], adaptive modified whale optimization algorithm (AMWOA) [32], spring search algorithm (SSA) [31], UVDA [30] and JAYA [33]. Table 2 shows that the proposed method is superior to the ACSA, AMWOA, SSA, UVDA and JAYA in most of the considered events in terms of percentage power loss reduction.

4.2 IEEE 69-bus RDN

IEEE 69-bus RDN consists of a base voltage of 12.66kV, real and reactive load size of 3801.89kW and 2694.1kVar, respectively. The fundamental loops obtained for the 69-bus RDN are shown in Table 3. The branches shown in the table give the boundary and limits of the possible open branches for each of the FLs.

Table 3. Fundamental loops (FLs) of the IEEE 69-bus RDN

FL Number	Branches
FL_1	3, 4, 5, 6, 7, 8, 9, 10, 35, 36, 37, 38, 39, 40, 41, 42, 69
FL_2	13, 14, 15, 16, 17, 18, 19, 20, 70
FL_3	3,4, 5, 6, 7, 8, 9, 10, 11, 12, 13, 14, 35, 36, 37, 38, 39, 40, 41, 42, 43, 44, 45, 71
FL_4	4, 5, 6, 7, 8, 46, 47, 48, 49, 52, 53, 54, 55, 56, 57, 58, 72
FL_5	9, 10, 11, 12, 13, 14, 15, 16, 17, 18, 19, 20, 21, 22, 23, 24, 25, 26, 52, 53, 54, 55, 56, 57, 58, 59, 60, 61, 62, 63, 64, 73

The results obtained for all the considered cases are summarized in Table 4. According to the table, the power loss (in kW) for the base case event is 225.00. The initial power loss (in kW) is significantly reduced from to 225.00 to 98.62, 69.44, 35.85, 39.63 and 35.27 for events 2, 3, 4, 5 and 6, respectively; and has a corresponding percentage power loss reduction (%PLR) of 56.17, 69.14, 84.07, 82.39 and 84.34. It is clearly seen from the table that the minimum voltage was significantly improved for all the considered events compared to the base case. The minimum voltage (bus location) was increased from 0.9098 (64) to 0.9428 (61), 0.9784 (65), 0.9753 (61), 0.9704 (63) and 0.9749 (61) for events 2 to 6, respectively. Similarly, the minimum voltage stability index(V_{min}), which is one of the performance evaluation metrics was improved from 0.6833 (65) to 0.7899 (61), 0.9163 (65), 0.9049 (61), 0.8854 (61) and 0.9039 (61) for events 2 to 6, respectively. A comparison of all the events reveals that event 6 gave the highest percentage power loss reduction demonstrating the efficiency of simultaneous RDNR and DG allocation.

Table 4. Summary and comparison of results for the various events for the 69-bus RDN

Event/item	Adaptive DOA	UVDA [30]	ACSA [24]	JAYA [33]	SSA [31]	AMWOA [32]
<u>Base case</u>						
TS	69 70 71 72 73	69 70 71 72 73	69 70 71 72 73	69 70 71 72 73	69 70 71 72 73	69 70 71 72 73
RP_{loss} (kW)	225.00	225.00	224.89	224.99	224.96	224.49
V_{min} (p.u.)	0.9098 (64)	0.9092 (65)	0.9092	0.9092	0.9092 (65)	--------
VSI_{min} (p.u)	0.6833(65)	--------	0.6859	0.6833	--------	0.6863
<u>RDNR only</u>						
TS	14 57 61 69 70	14 58 61 69 70	14 57 61 69 70	14 56 61 69 70	14 58 61 69 70	14 57 61 69 70
RP_{loss} (kW)	98.62	98.58	98.59	99.59	98.63	98.41
%PLRI	**56.17**	**56.17**	**56.16**	**55.74**	**56.15**	**56.16**
V_{min} (p.u.)	0.9428 (61)	0.9495 (61)	0.9495	0.9428	0.9492 (61)	--------
VSI_{min} (p.u)	0.7899 (61)	--------	0.8414	0.7898	--------	0.8415

DG only						
TS	69 70 71 72 73	69 70 71 72 73	69 70 71 72 73	69 70 71 72 73	69 70 71 72 73	69 70 71 72 73
DG size in kW (bus no)	519 (11) 392 (18) 1701 (61)	604 (11) 417 (17) 1410 (61)	602.2 (11) 380.4 (18) 2000 (61)	595.8 (11) 381.9 (19) 2000 (61)	527 (10) 380 (17) 1718 (60)	602.2 (11) 589.3 (18) 145.1 (64)
RP_{loss} (kW)	69.44	72.63	72.44	72.44	69.41	71.41
%PLRI	**69.14**	**67.72**	**67.79**	**67.80**	**69.14**	**68.19**
V_{min} (p.u.)	0.9784 (65)	0.9688 (65)	0.9890	0.9890	0.9789 (65)	-------
VSI_{min} (p.u)	0.9163 (65)	-------	0.9546	0.9569	-------	0.9656
DG after RDNR						
TS	14 57 61 69 70	14 58 61 69 70	14 57 61 69 70	14 61 64 69 70	14 58 61 69 71	14 57 61 69 70
DG size in kW (bus no)	540 (11) 574 (27) 1445 (61)	620 (11) 1378 (61) 722 (64)	368.6 (12) 1725.4 (61) 466.6 (64)	530.9 (11) 1743.4 (61) 489.7 (64)	538 (11) 566 (27) 1434 (61)	1201.6 (33) 818.1 (32) 484.9 (67)
RP_{loss} (kW)	35.85	37.84	37.23	37.53	35.54	35.62
%PLRI	**84.07**	**83.18**	**83.45**	**83.32**	**84.20**	**84.17**
V_{min} (p.u.)	0.9753 (61)	0.9801 (61)	0.9870	0.9810	0.9812 (61)	-------
VSI_{min} (p.u)	0.9049 (61)	-------	0.9390	0.9251	-------	0.9520
RDNR after DG						
TS	12 57 64 68 70	-------	14 58 64 69 70	13 56 64 69 70	14 56 62 69 71	-------
DG size in kW (bus no)	519 (11) 392 (18) 1701 (61)	-------	602.2 (11) 380.4 (18) 2000 (61)	595.8 (11) 381.9 (19) 2000 (61)	527 (10) 380 (17) 1718 (60)	-------
RP_{loss} (kW)	39.63	-------	41.13	41.57	45.18	-------
%PLRI	**82.39**	-------	**81.71**	**81.52**	**79.91**	-------
V_{min} (p.u.)	0.9704 (63)	-------	0.9828	0.9753	0.9747 (64)	-------
VSI_{min} (p.u)	0.8854(61)	-------	0.9260	0.9049	-------	-------
RDNR and DG						
TS	14 57 61 69 70	14 58 63 69 70	14 58 61 69 70	10 18 14 58 63	14 58 63 69 70	8 17 57 62 71
DG size in kW (bus no)	540 (11) 1432 (61) 489 (64)	538 (11) 673 (17) 1472 (61)	1724 (61) 553.6 (65) 541.3 (11)	1790 (62) 477.3 (65) 622.6 (68)	650 (11) 490 (27) 1467.5 (61)	1694.3 (18) 950.1 (36) 439.8 (61)
RP_{loss} (kW)	35.27	37.11	37.02	44.04	35.81	35.25
%PLRI	**84.34**	**83.51**	**83.54**	**80.42**	**83.20**	**84.30**
V_{min} (p.u.)	0.9749 (61)	0.9816 (63)	0.9869	0.9807	0.9808 (61)	-------
VSI_{min} (p.u)	0.9039 (61)	-------	0.9433	0.9239	-------	0.9433

The voltage profiles and voltage stability indices (VSIs) for all the considered events are displayed in Figures 8 and 9, respectively.

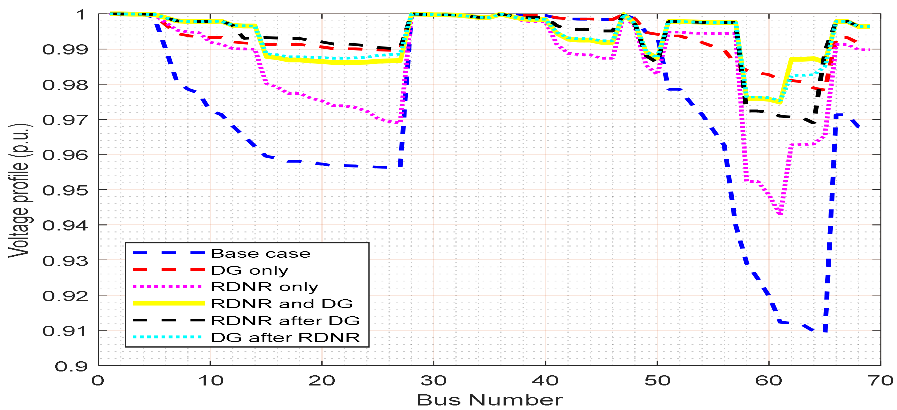

Figure 8.

Voltage profile of events 1 – 6 for 69-bus RDN

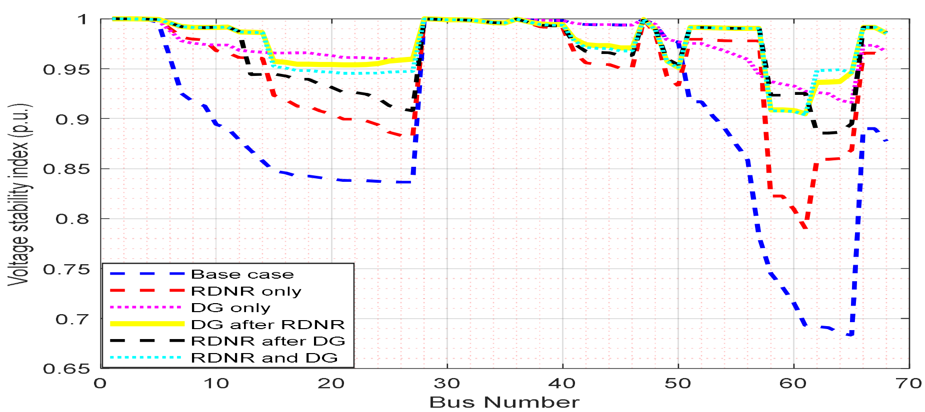

Figure 9. Voltage stability indices of events 1 – 6 for 69-bus RDN

It is clear from the figures that the bus voltages and voltage stability indices (VSIs) are significantly improved after simultaneous RDNR and DG allocation.

Advances In Multidisciplinary & Scientific Research
AIMS Research Journal
A Multidisciplinary & Interdisciplinary Journal
Volume 8, No 2, June 2022 Series

The convergence characteristics of events 2 to 6 are illustrated in Figure 10.

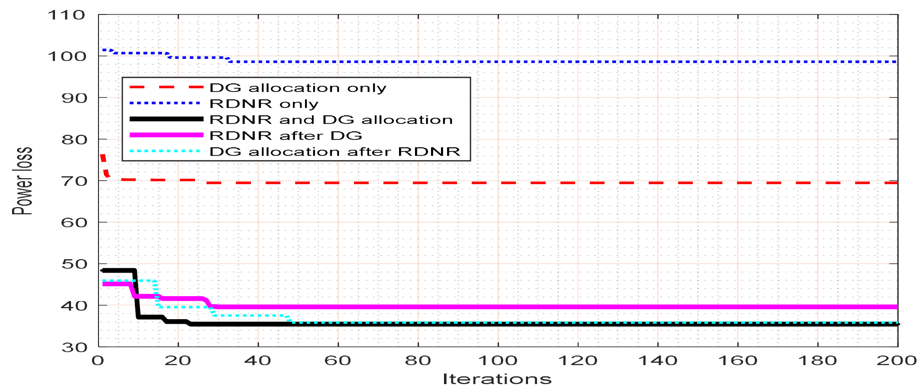

Figure 10. Convergence characteristics of events 2 – 6 for 69-bus RDN

The performance of the adaptive DOA technique is objectively compared with the results of recent literatures that considered the similar events as presented in Table 4. The proposed method is validated using previously reported results of other techniques such as adaptive cuckoo search algorithm (ACSA) [24], adaptive modified whale optimization algorithm (AMWOA) [32], spring search algorithm (SSA) [31], UVDA [30] and JAYA [33]. Table 4 shows that the proposed method is superior to the ACSA, AMWOA, SSA, UVDA and JAYA in most of the events in terms of percentage power loss reduction. It can be seen that event 6 (simultaneous RDNR and DG allocation) has the least power loss closely followed by events 4 and 5.

5. CONCLUSION

In this paper, an adaptive dingo optimization algorithm (DOA) is presented to optimize simultaneous radial distribution network reconfiguration (RDNR) and distributed generation allocation with the aim of reducing the power loss of the of radial distribution networks. The proposed method utilized graph theory to predetermine the tie switches in the search space in order to significantly minimize the infeasible configurations in the optimization process, and also adapt it to perform the radial constraint check of the generated configurations. In a bid to establish the effectiveness of the proposed method, six different events were considered such as base case without reconfiguration and DG allocation, reconfiguration only,

DG allocation only, DG allocation after reconfiguration, reconfiguration after DG allocation and simultaneous reconfiguration and DG allocation. The adaptive DOA is tested on standard IEEE 33 and 69-bus RDNs. The simulation results reveal that simultaneous RDNR and DG allocation gave the least power loss compared to the other considered events. The efficacy of the proposed method is further validated with comparison of the observed simulation results with the previously reported results of competitive algorithms available in literatures such as UVDA, ACSA, JAYA, SSA and AMWOA. The comparative study shows that the adaptive DOA outperform these algorithms in most of the considered scenarios.

REFERENCES

[1] A. A. Sallam and O. P. Malik, "Electric Dsitribution System Modeling," IEEE press, Piscataway, NJ, 2011.

[2] W. H. Kersting, "Distribution System Modeling and Analysis," CRC Press, New York, 2002.

[3] R. S. Rao, S. V. L. Narasimham and M. Ramalingaraju, "Optimal Capacitor Placement in a Radial Distribution System using Plant Growth Simulation Algorithm," International Journal of Electrical Power & Energy Systems, Vol. 33, Issue 5, pp. 1133-1139, June 2011, https://doi.org/10.1016/j.ijepes.2010.11.021

[4] P. V. Babu and S. P. Singh, "Optimal Placement of DG in Distribution Network for Power Loss Minimization using NLP & PLS Technique," Energy Procedia, Vol. 90, p. p441-454, Dec. 2016, https://doi.org/10.1016/j/.egypro.2016.11.211

[5] S. A. Taher and M. H. Karimi, "Optimal Reconfiguration and DG Allocation in Balanced and Unbalanced Distribution Systems," Ain Shams Engineering Journal, 5(3), pp. 735-749, Sept. 2014, https://doi.org/10.1016/j.asej.2014.03.009.

[6] T. S. Tawfeek, A. H. Ahmed and S. Hassan, "Analytical and particle swarm optimization algorithms for optimal allocations of four different distributed generation types in radial distribution networks," Energy Procedia, 153 pp. 86-94, Oct. 2018, https://doi.org/10.1016/j.egypro.2018.10.030

[7] K. S. Sambaiah and T. Jayabarathi, "Optimal Reconfiguration and Renewable Distributed Generation Allocation in Electric Distribution System," International Journal of Ambient Energy, Vol. 42, Issue 9, pp. 1018-1031, Mar. 2019, https://doi.org/10.1080/01430750.2019.1583604

[8] W. Guan, Y. Tan, H. Zhang and J. Song, "Distribution System Feeder Reconfiguration Considering Different Model of DG Sources," International Journal of Electrical Power & Energy Systems 2015; Vol. 68, pp. 210–221, June 2015, https://doi:10.1016/j.ijepes.2014.12.023

[9] M. Esmaeili, M. Sedighizadeh and M. Esmaili, "Multi-objective Optimal Reconfiguration and DG (Distributed Generation) Power Allocation in Distribution Networks using Big Bang-Big Crunch Algorithm Considering Load Uncertainty," Energy, Vol. 103, pp. 86-99, 2016, https://doi:10.1016/j.energy.2016.02.152

[10] S. R. Tuladhar, J. G. Singh and W. Ongsakul, "Multi-Objective Approach for Distribution Network Reconfiguration with Optimal DG Power Factor using NSPSO," IET Generation, Transmission & Distribution 2016; 10 (12), pp. 2842-2851, June 2016.

[11] A. Jafar-Nowdeh, M. Babanezhad, S. Arabi-Nowdeh, A. Naderipour, H. Kamyab, Z. Abdul-Malek and V. K. M. Ramachandara, "Meta-heuristic matrix moth-flame algorithm for optimal reconfiguration of distribution networks and placement of solar and wind renewable sources considering reliability," Environmental Technology & Innovation, Vol. 20, Nov. 2020, https://doi.org/10.1016/j.eti.2020.101118

[12] N. Kanwar, N. Gupta, K. R. Niazi and A. Swarnkar, "Optimal Allocation of DGs and Reconfiguration of Radial Distribution Systems using an Intelligent Search-based TLBO, "Electric Power Components and Systems," Vol. 45, Issue 5, pp. 476–490, Feb. 2017, https://doi.org/10.1080/15325008.2016.1266714.

[13] I. Quadri, S. Bhowmick and D. Joshi, "A multi-objective approach to maximize loadability of distribution networks by simultaneous reconfiguration and allocation of distributed energy resources," IET Generation, Transmission & Distribution, Oct. 2018, https://doi.org/10.1049/iet-gtd.2018.5618

[14] P. P. Biswas, P. N. Suganthan and G. A. J. Amaratunga, "Distribution Network Reconfiguration Together with Distributed Generator and Shunt Capacitor Allocation for Loss Minimization," IEEE Congress on Evolutionary Computation (CEC), Oct. 2018, https://doi.org/10.1109/cec.2018.8477894

[15] U. Raut and S. Mishra, "An improved Elitist–Jaya algorithm for simultaneous network reconfiguration and DG allocation in power distribution systems," Renewable Energy Focus, 30 (2), pp. 92–106, Sept. 2019, https://doi.org/10.1016/j.ref.2019.04.001

[16] A. M. Shaheen, A. M. Elsayed, R. A. El-Sehiemy and A. Y. Abdelaziz, "Equilibrium optimization algorithm for network reconfiguration and distributed generation allocation in power systems," Applied Soft Computing, Vol. 98, Jan. 2021, https://doi.org/10.1016/j.asoc.2020.106867

[17] M. A. Abdelkader, Z. H. Osman and M. A. Elshahed, "New analytical approach for simultaneous feeder reconfiguration and DG hosting allocation in radial distribution networks," Ain Shams Engineering Journal, Vol. 12, Issue 2, pp. 1823-1837, June 2021, https://doi.org/10.1016/j.asej.2020.09.024

[18] U. Raut and S. Mishra, "An improved sine-cosine algorithm for simultaneous network reconfiguration and DG allocation in power distribution systems," Applied Soft Computing, Vol. 92, July 2020, https://doi.org/10.1016/j.asoc.2020.106293

[19] A. M. Shaheen, A. M. Elsayed, R. A. El-Sehiemy, S. Kamel and S. S. M. Ghoneim, "A modified marine predators optimization algorithm for simultaneous network reconfiguration and distributed generator allocation in distribution systems under different loading conditions," Engineering Optimization, Vol. 54, Issue 4, pp. 687-708, Apr. 2021, https://doi.org/10.1080/0305215x.2021.1897799

[20] U. Raut and S. Mishra, "Enhanced sine–cosine algorithm for optimal planning of distribution network by incorporating network reconfiguration and distributed generation," Arabian Journal for Science and Engineering, 46 (2), pp. 1029-1051, Aug. 2020, https://doi.org/10.1007/s13369-020-04808-9

[21] V. K. Thunuguntla and S. K. Injeti, "Butterfly optimizer assisted Max–Min based multi-objective approach for optimal connection of DGs and optimal network reconfiguration of distribution networks," Journal of Electrical Systems and Information Technology, 9 (8), 1-25. Dec. 2022, https://doi.org/10.1186/s43067-022-00049-y

[22] A. Shaheen, A. Elsayed, A. Ginidi, R. El-Sehiemy and E. Elattar, “Reconfiguration of electrical distribution network-based DG and capacitors allocations using artificial ecosystem optimizer: Practical case study,” Alexandria Engineering Journal, Vol. 61, Issue 8, pp. 6105-6118, Aug. 2022, https://doi.org/10.1016/j.aej.2021.11.035

[23] A. Bagheri, M. Bagheri and A. Lorestani, “Optimal reconfiguration and DG integration in distribution networks considering switching actions costs using tabu search algorithm,” Journal of Ambient Intelligence and Humanized Computing, 12 (21) pp. 7837-7856, Sept. 2020, https://doi.org/10.1007/s12652-020-02511-z

[24] T. T. Nguyen, A. V. Truong and T. A. Phung, “A novel method based on adaptive cuckoo search for optimal network reconfiguration and distributed generation allocation in distribution network,” International Journal of Electrical Power & Energy Systems, Vol. 78, pp. 801-815, June 2016, https://doi.org/10.1016/j.ijepes.2015.12.030

[25] R. S. Rao, K. Ravindra, K. Satish and S. V. L. Narasimham, “Power Loss Minimization in Distribution System Using Network Reconfiguration in the Presence of Distributed Generation,” IEEE Transactions on Power Systems, Vol. 28, Issue 1, pp. 317–325, Feb. 2013, https://doi.org/10.1109/tpwrs.2012.2197227

[26] A. M. Imran, M. Kowsalya and D. P. Kothari, “A novel integration technique for optimal network reconfiguration and distributed generation placement in power distribution networks,” International Journal of Electrical Power & Energy Systems, Vol. 63, pp. 461–472, Dec. 2014, https://doi.org/10.1016/j.ijepes.2014.06.011

[27] M. G. Naguib, W. A. Omran, and H. E. A. Talaat, “Optimal reconfiguration and DG allocation in active distribution networks using a probabilistic approach,” IEEE PES Innovative Smart Grid Technologies Conference Europe (ISGT-Europe), Sept. 2017, https://doi.org/10.1109/ISGTEurope.2017.8260224

[28] R. Rajaram, K. S. Kumar and N. Rajasekar, “Power system reconfiguration in a radial distribution network for reducing losses and to improve voltage profile using modified plant growth simulation algorithm with Distributed Generation (DG),” Energy Reports; Vol. 1, pp. 116–122. Nov. 2015, https://doi.org/10.1016/j.egyr.2015.03.002

[29] M. Ahanch, M. S. Asasi and M. S. Amiri, “A Grasshopper Optimization Algorithm to Solve Optimal Distribution System Reconfiguration and Distributed Generation Placement Problem,” 2017 IEEE 4th International Conference on Knowledge-Based Engineering and Innovation (KBEI), Dec. 2017, https://doi.org/10.1109/kbei.2017.8324880

[30] A. Bayat, “Uniform voltage distribution based constructive algorithm for optimal reconfiguration of electric distribution networks. Electric Power Systems Research,” Vol. 104, Nov. 2013, pp. 146-155, https://doi.org/10.1016/j.epsr.2013.06.010

[31] K. S. Sambaiah and T. Jayabarathi, "Optimal Reconfiguration and Renewable Distributed Generation Allocation in Electric Distribution Systems," International Journal of Ambient Energy, Vol. 42, Issue 9, pp. 1018-1031, Feb. 2019, https://doi.org/10.1080/01430750.2019.1583604

[32] A. Uniyal and S. Sarangi, "Optimal network reconfiguration and DG allocation using adaptive modified whale optimization algorithm considering probabilistic load flow," Electric Power Systems Research, Vol. 192, Mar. 2021, https://doi.org/10.1016/j.epsr.2020.106909

[33] M. S. Rawat and S. Vadhera, "Heuristic optimization techniques for voltage stability enhancement of radial distribution network with simultaneous consideration of network reconfiguration and DG sizing and allocations," Turkish Journal of Electrical Engineering & Computer Science, Vol. 27, Issue 1, pp. 330-345, Jan. 2019, https://doi.org/10.3906/elk-1806-181

[34] M. F. Abd El-salam, E. Beshr and M. B. Eteiba, "A New Hybrid Technique for Minimizing Power Losses in a Distribution System by Optimal Sizing and Siting of Distributed Generators with Network Reconfiguration," Energies, Vol. 11, Issue 12, Nov. 2018, https://doi.org/10.3390/en11123351

[35] E. S. Ali, S. M. Abd Elazim and A. Y. Abdelaziz, "Improved Harmony Algorithm and Power Loss Index for optimal locations and sizing of capacitors in radial distribution systems," International Journal of Electrical Power & Energy Systems, Vol. 80, pp. 252–263, Sept. 2016, https://doi.org/10.1016/j.ijepes.2015.11.085

[36] W. S. Tan, M. Y. Hassan, M. S. Majid and H. A. Rahman, "Allocation and sizing of DG using cuckoo search algorithm," 2012 IEEE International Conference on Power and Energy (PECon), Dec. 2012, https://doi.org/10.1109/PECon.2012.6450192

[37] A. K. Bairwa, S. Joshi and D. Singh, "Dingo optimizer: A Nature-Inspired Metaheuristic Approach for Engineering Problems," Mathematical Problems in Engineering, pp. 1-12, June 2021, https://doi.org/10.1155/2021/2571863

[38] M. Mohammadi, A. M. Rozbahani and S. Bahmanyar, "Power loss reduction of distribution systems using BFO based optimal reconfiguration along with DG and shunt capacitor placement simultaneously in fuzzy framework," Journal of Central South University. 24 (1), pp. 90-103, Jan. 2017, https://doi.org/10.1007/s11771-017-3412-1

[39] N. Gupta, A. Swarnkar, K. R. Niazi and R. C. Bansal, "Multi-objective reconfiguration of distribution systems using adaptive genetic algorithm in fuzzy framework," IET Generation, Transmission & Distribution, 4(12), pp. 1288-1298, Dec. 2010, https://doi.org/10.1049/iet-gtd.2010.0056

[40] E. Dolatdar, S. Soleymani and B. Mozafari, "A New Distribution Network Reconfiguration Approach using a Tree Model," International Journal of Computer and Information Engineering, 3(10), pp. 2480-2487, Oct. 2009, https://doi.org/10.5281/ZENODO.1057593

[41] M. E. Baran and F. F. Wu, "Network econfiguration in distribution systems for loss reduction and load balancing," IEEE Power Engineering Review, Vol. 4, Issue 2, pp. 1401-1407, Apr.1989, https://doi.org/10.1109/61.25627
[42] H. D. Chiang and R. Jean-Jumeau, "Optimal network reconfigurations in distribution systems. II. Solution algorithms and numerical results," IEEE transactions on Power delivery. 1990; Vol. 5, Issue 3, pp. 1568-1574, July 1990, https://doi.org/10.1109/61.58002